

PAPER

Modification of toroidal flow velocity through momentum Injection by compact torus injection into the STOR-M tokamak

To cite this article: A. Rohollahi *et al* 2017 *Nucl. Fusion* **57** 056023

View the [article online](#) for updates and enhancements.

You may also like

- [Modification of plasma rotation with resonant magnetic perturbations in the STOR-M tokamak](#)
S Elgrw, Y Liu, A Hirose et al.
- [Effects of lithium coating of the chamber wall on the STOR-M tokamak discharges](#)
A. Rohollahi, S. Elgrw, A. Mossman et al.
- [Tangential and Vertical Compact Torus Injection Experiments on the STOR-M Tokamak](#)
Xiao Chijin, D Liu, S Livingstone et al.

Modification of toroidal flow velocity through momentum Injection by compact torus injection into the STOR-M tokamak

A. Rohollahi¹, S. Elgriw¹, D. Basu¹, S. Wolfe², A. Hirose¹ and C. Xiao¹

¹ Plasma Physics Laboratory, University of Saskatchewan, Saskatoon, Canada

² Plasmionique Inc., Varennes, Canada

E-mail: chijin.xiao@usask.ca

Received 16 December 2016, revised 13 February 2017

Accepted for publication 7 March 2017

Published 28 March 2017



Abstract

In the Saskatchewan torus-modified (STOR-M) tokamak, tangential compact torus injection (CTI) experiments have been performed with normal (counter-clockwise, CCW, top view) and reversed (clockwise, CW, top view) plasma current directions while the compact torus (CT) injection direction remains in the CCW direction. The intrinsic toroidal flow direction reverses when the discharge current is reversed. However, the change in the toroidal flow direction is always toward the CTI direction (CCW). It has been determined that the momentum in high density and high velocity CT is more than ten times larger than the intrinsic toroidal rotation momentum in the typical STOR-M plasma. Therefore, the modification of the plasma toroidal rotation velocity is attributed to momentum transfer from CT to the tokamak discharge.

Keywords: compact torus injection, toroidal flow, momentum, ion doppler spectroscopy, impurity, flow shear

(Some figures may appear in colour only in the online journal)

1. Introduction

Compact torus injection (CTI) is one of the proposed fueling methods for a magnetic fusion reactor and the only candidate for direct core fueling of large tokamaks [1–3]. A compact torus (CT) is a magnetized plasmoid with approximately equal toroidal and poloidal magnetic fields. CTs can be formed and accelerated inside a coaxial gun and can withstand high acceleration force to reach a high velocity [4]. CTI has the potential to control plasma pressure profile to optimise bootstrap current through precise control of the amount and deposition position of the fuel [5]. Also, CTI can be operated repetitively with high repetition frequency to provide a continuous and consistent fueling for fusion reactors [6]. CTI has been considered as a means to inject momentum into the tokamak plasma to control the toroidal flow. Toroidal flow in tokamaks plays an important role in improvement of plasma confinement, suppression of magnetohydrodynamic (MHD) modes, and mitigation of plasma disruptions. Plasma flow and its shear in tokamak discharges have other beneficial effects

including suppression of turbulence, control of the resistive wall modes, maintaining high β as well as enhancing tolerance to the unavoidable error fields which may cause mode locking and even major disruptions [7, 8]. Unbalanced neutral beam injection (NBI) is the common method to induce a substantial plasma flow in large tokamaks. NBI requires a large amount of stored energy to accelerate particles to a sufficiently high velocity in order to inject momentum into the tokamak plasma in addition to plasma heating [9]. The Saskatchewan torus-modified (STOR-M) tokamak is equipped with a tangential compact torus injector and a set of ($n = 1$, $m = 2$) helical coils used to induce resonant magnetic perturbations (RMP) to suppress magnetic perturbations in the STOR-M plasma [10]. Suppression of the $m = 2$ MHD mode and transition to improved plasma confinement (H-mode) after tangential CTI have been observed [7]. It has also been recently found that the toroidal flow velocity can be modified by tangential CTI [5] and RMP fields [11] along with suppression of MHD fluctuations. In both RMP and tangential CTI cases, the change of the toroidal flow velocity was in the counter-clockwise

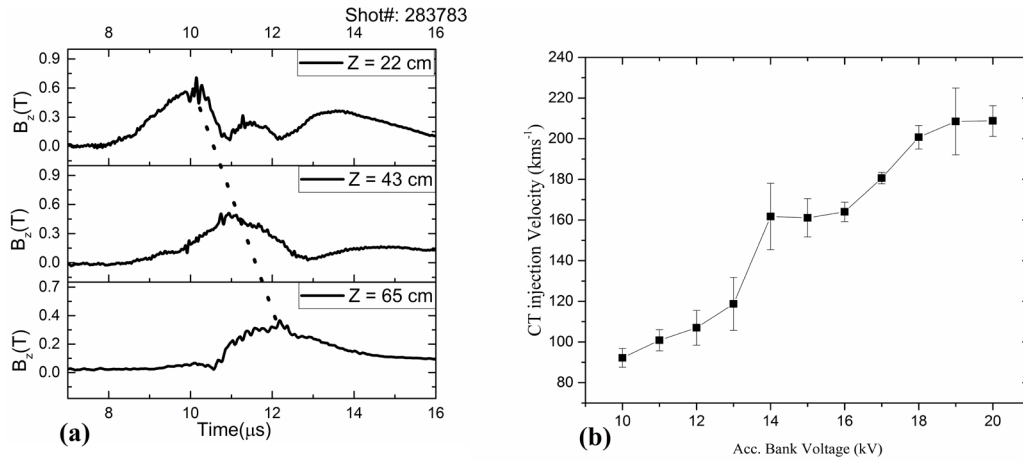


Figure 1. (a) CT poloidal (axial) magnetic fields measured at three axial locations along the acceleration electrode. (b) The CT velocity versus the acceleration bank voltage averaged over 45 CTs for each of the voltages.

(CCW, top view) direction, coincide with both CT injection direction and the plasma current direction. Since CT injection also suppresses the magnetic fluctuations in STOR-M [7], it was difficult to conclude whether the flow velocity modification was completely associated with suppression of magnetic fluctuations or modifications of profiles of the plasma parameters, similar to the RMP case, or also due to CT momentum injection. For this reason, the direction of plasma current discharge was reversed in the recent experiments from the CCW to CW direction. As expected, the intrinsic flow velocity direction was reversed by changing the direction of plasma discharge current. Since the RMP field is no longer resonant with the magnetic island due to the change of the plasma current direction, non-resonant RMP induced a much smaller modification of toroidal flow velocity towards the co-current direction (now CW direction) [11].

This paper will focus on the experimental observations of the modification of the toroidal flow velocity due to tangential CTI with reversed plasma current direction (CW) and compare the results with those previously observed with normal plasma current direction (CCW) after CTI. It will be concluded that the modification induced by CTI is primarily due to injection of CT momentum into the STOR-M discharge.

2. Experimental setup

The STOR-M tokamak ($R/a = 0.46/0.12$ cm, $B_t = 0.65$ T, $I_p = 22$ kA) is a small research tokamak at the University of Saskatchewan equipped with the University of Saskatchewan compact torus injector (USCTI). The unique interface between USCTI and STOR-M allows USCTI to inject a CT tangentially in the toroidal direction into the STOR-M tokamak at the controllable injection velocities $v = 90\text{--}210$ km s $^{-1}$ [12]. USCTI has a coaxial configuration with formation, compression, and acceleration sections. Two similar capacitor banks (20 μF , up to 30 kV) are used for CT formation and acceleration. A cone-shaped compressor reduces the diameter of the CT from 15 cm in the formation region to 10 cm in the acceleration region. The diameter of the inner acceleration electrode is 3.6 cm at the straight accelerator region. An array

of four magnetic probes mounted on the inner surface of the outer electrode is used to measure the poloidal and toroidal magnetic field in USCTI at axial locations $z = 0, 22, 43.5, 65$ cm. The injection velocity of CT can be calculated from the time delay of the magnetic field signals measured at three axial locations in the straight accelerator region. A He-Ne laser interferometer is used to measure the CT density at the end of the acceleration section. The typical CT plasma density is about $n_{\text{CT}} = 3 \times 10^{15}$ cm $^{-3}$. The mass in the CT plasma is about 0.5 μg which is 50% of the total mass (1 μg) in the STOR-M plasma. The injection velocity of CT can be controlled by the acceleration bank voltage.

To Minimize the impurities carried by CTs, the injector electrodes have been baked for a week under a high vacuum ($p = 8.2 \times 10^{-8}$ torr), and 400 CT discharges have been performed to do extra cleaning. The CTI electrodes are coated by tungsten to reduce the surface erosion. It has been reported previously, the injected CT with a high injection velocity does not carry the heavy metallic impurities as reported in [3].

A typical set of waveforms of three magnetic probe signals is shown in figure 1(a). The dashed line indicates the delay of the magnetic field signal measured when the CT is pushed downstream between the coaxial acceleration electrodes. Figure 1(b) shows the calculated CT velocity as a function of the acceleration bank voltage. In figure 1(b), each CT injection velocity data point is calculated by averaging over 45 similar CT discharges. For the acceleration bank voltages lower than 18 kV ($V_{\text{acc}} \leq 18$ kV), the injection velocity increases with acceleration bank voltage. For V_{acc} at 18 kV and 20 kV, the maximum achievable injection velocity for the USCTI is $v_{\text{inject}} = 210$ km s $^{-1}$ for this particular set of CT discharge parameters. The CT velocity increase appears to slow down similar to what was observed for voltages 14–15 kV. Due to limitations of the power supply currently used, it has not attempted to further increase acceleration bank voltage to investigate whether CT velocity can be further increased at higher acceleration bank voltages.

An ion Doppler spectroscopy (IDS) system is installed on the STOR-M tokamak to measure the toroidal flow velocity. The IDS system may also be able to measure the ion

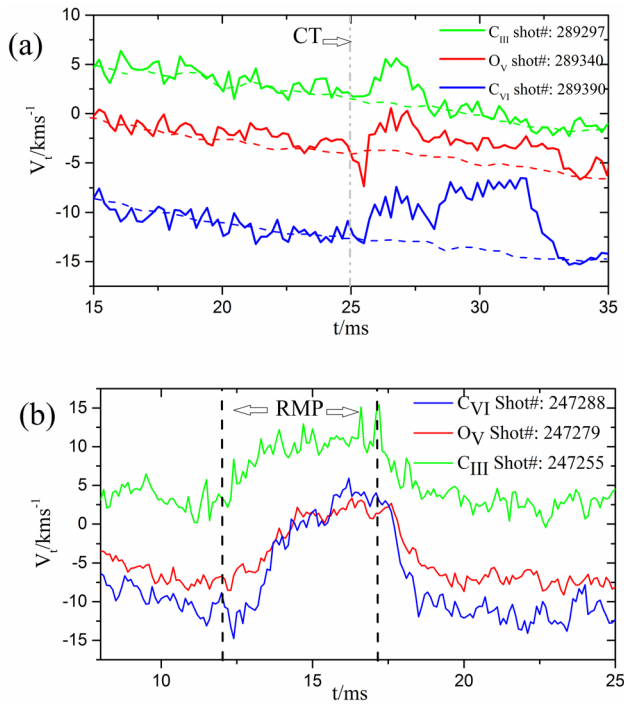


Figure 2. Modification of toroidal flow velocities of impurity ions at $r = 0$ cm (C_{VI} , blue), $r = 3$ cm (O_V , red) and at $r = 7$ cm (C_{III} , green) by application of RMP (a) and CTI (b). The plasma current is in the CCW direction for both the RMP and CTI cases.

temperature in fusion devices based on broadening of spectral lines [13, 14]. Three bright line emission spectra from STOR-M, C_{III} (4647.4 Å), C_{VI} (5290.5 Å) and O_V (2728 Å), are selected because they are in different ionization stage and are emitted from different radial locations of the tokamak plasma due to the peaked temperature profile expected in the STOR-M plasma. The radial profile of the brightness measurements from a series of vertical chords and the subsequent inversion show that C_{III} emission comes from the region of the tokamak plasma near $r = 7$ cm and C_{VI} from the core ($r = 0$ cm). The most probable location for the O_V emission is around $r = 3$ cm. The IDS system for the STOR-M tokamak has a velocity resolution of $v \approx 1\text{--}2$ km s $^{-1}$ [5], determined by the range of the fluctuating spectral peak locations when the line of sight of the IDS system is in the minor radial direction.

While maintaining the toroidal field in the CCW direction (top view), the toroidal plasma current direction can be easily reversed by changing the current direction in the primary windings. The horizontal position feedback control system was already designed for alternating current operation in STOR-M and is able to handle the normal (CCW) and reversed (CW) tokamak discharge current directions in STOR-M without any further modifications [15].

3. Experimental results

The baseline measurements of the plasma flow for normal (CCW) discharge current direction are shown in figure 2 with RMP and CT injection in the co-current (CCW) direction. The RMP current ($I_{RMP} = 600$ A) is switched on during the time $t = 12\text{--}17$ ms as shown in figure 2(a). The CT is injected

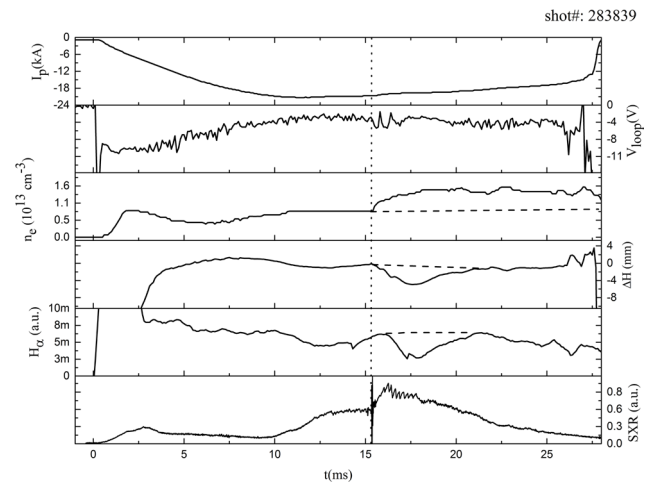


Figure 3. Discharge waveforms of discharge (283839) with CT injected at 15.5 ms. The plasma current is in the CW direction. Parameters shown are plasma current, loop voltage, line-averaged electron density, plasma horizontal position, H_α emission and SXR emission. The CT trigger time is indicated by the dashed vertical line. The horizontal dashed lines show the averaged values over 45 STOR-M discharges without CTI.

at $t = 25$ ms as shown in figure 2(b). The intrinsic flow is in the co-current direction (positive value, CCW) at $r = 7$ cm (C_{III}) and in the counter-current direction (negative value, CW) at $r = 4$ cm (O_V) and $r = 0$ cm (C_{VI}), indicating a significant flow shear across the minor radius. The plasma flow changes towards the co-current direction after RMP and CTI. It is noted that the CT carries a momentum approximately ten times higher than that of the STOR-M plasma in the toroidal direction based on the measured velocity and the mass of CT and the baseline STOR-M plasma toroidal rotation speed. Since the velocity changes towards the CT injection direction at all the locations regardless the baseline velocity directions, it tends to suggest that the modification of the toroidal flow in the co-injection direction is due to the transfer of CT momentum to the STOR-M discharge. However, this is not conclusive since the RMP experiments without direct particle momentum injection resulted in a flow modification similar to the case with CTI as shown in figure 2.

It is envisaged that the intrinsic toroidal flow velocity direction is closely related to poloidal field direction through $\vec{E}_r \times \vec{B}_\theta$ and $(-\nabla p) \times \vec{B}_\theta$. In the recent experiments, the discharge current direction in STOR-M was reversed in an attempt to reverse the intrinsic toroidal flow directions and CT injection experiments were repeated. Since the helical RMP coil is no longer resonant with the tokamak magnetic field direction, non-resonant RMP has a little effect on the toroidal flow velocity as reported earlier [10]. It should be stressed that the CT injection remains in the CCW direction. The following discussion will be mainly on CTI experiments with reversed discharge current in STOR-M.

The typical waveforms of a STOR-M discharge with a CT injected at $t = 15.5$ ms are illustrated in figure 3 for the reversed plasma current configuration as indicated by the negative plasma current value. The plasma current is ramped up to -19 kA in 10 ms and flat top duration is about 17 ms. During the flat top, the line-averaged electron density of

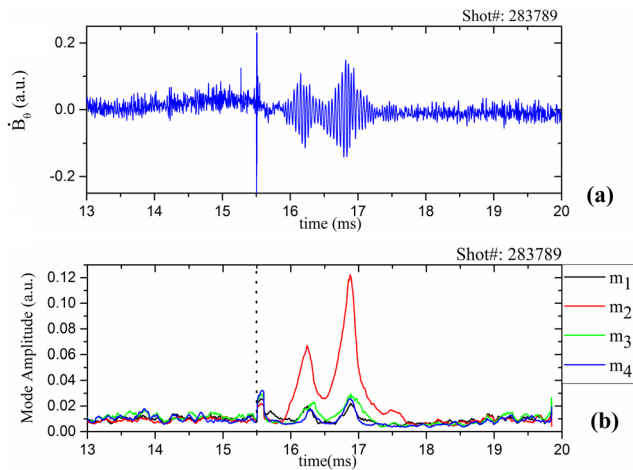


Figure 4. Magnetic fluctuation of poloidal field measured by Mirnov coil (a) and magnitude of $m = 1$ (black), $m = 2$ (red), $m = 3$ (green) and $m = 4$ (blue) constructed by Fourier series analysis (b).

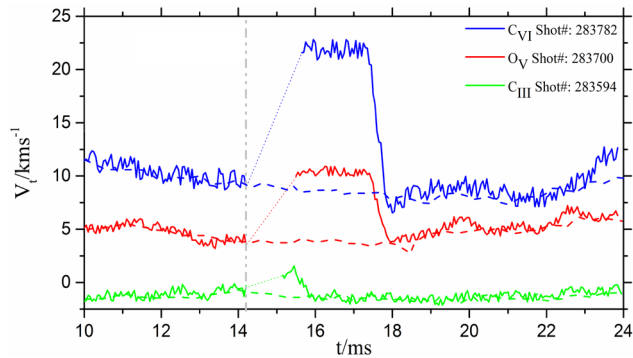


Figure 5. Modification of toroidal flow velocities of impurity ions at $r = 0$ cm (C_{VI} , blue), $r = 3$ cm (O_V , red) and at $r = 7$ cm (C_{III} , green) for the reversed plasma discharge current direction. The dotted lines in the curves indicate the time span when the flow measurement was impeded due to noises. The dashed lines show the flow velocity averaged over ten typical discharges without CTI.

plasma, measured by a 4 mm microwave interferometer, is $n_e = 0.9 \times 10^{13} \text{ cm}^{-3}$ which decays slowly. As shown in the third panel in figure 3, the line-average electron density of plasma increases considerably after CTI due to the fuelling effect of CTI and/or improved confinement. The density reaches its maximum value $n_e = 1.26 \times 10^{13} \text{ cm}^{-3}$ at $t = 18$ ms. The density increase rate after CTI is approximately $1.26 \times 10^{15} \text{ cm}^{-3} \text{ s}^{-1}$. As shown in the fourth panel, the plasma position moves outward from $\Delta H = 0$ mm to $\Delta H = -5$ mm when the plasma density starts to increase after CTI injection. This outward displacement is likely due to an increase in the thermal energy in the STOR-M discharge after CT injection [16]. The horizontal position control system for STOR-M is able to restore the plasma position within 2 ms to its initial position. As illustrated in figure 3, the H_α radiation intensity decreases by about 50% after CTI for a short period and returns to its initial level after 2.5 ms. The decrease and increase in H_α radiation resemble the L-H and H-L transitions, respectively. Improvement of the particle confinement and an increase in the global energy confinement in the STOR-M tokamak after CTI have been reported previously [16] and the

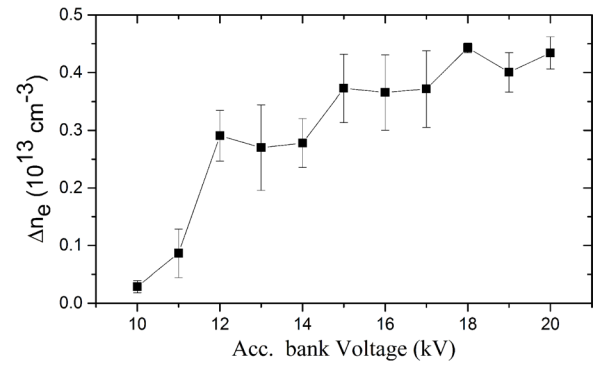


Figure 6. The injection velocity of CT versus acceleration bank voltage averaged over 45 CTs for each of the voltages.

recent results confirm those observations. The second trace of figure 3 shows that the average plasma loop voltage remains constant, after CTI. As there is no change in the plasma current due to CTI, the Spitzer resistivity of the plasma remains unchanged after CTI. Also, it has been reported previously that CTI does not increase the plasma temperature [2]. Therefore, the Z_{eff} of the plasma does not change significantly due to CTI. It should be pointed out that STOR-M is also equipped with a soft x-ray (SXR) camera system. As shown in the last trace of figure 3, the SXR emission from the plasma core increases after CTI to more than two times compared to the SXR emission before CTI. The SXR emission signal has a fast rise after CTI but decays slowly afterwards even though the density remains constant for a longer period of time. The SXR radiation consists of the bremsstrahlung from free electrons and recombination radiation of partially ionized impurities. The SXR radiation depends on the density, temperature, impurities and effective ionic charge. The exact mechanism causing the increase in the SXR emission intensity after CTI has not been clearly identified in this experimental campaign and remains for future investigation.

Injection of CTs into the CW plasma current excites magnetic fluctuations, as shown in figure 4(a). The amplitudes of $m = 1, 2, 3$ and 4 modes calculated by the spatial Fourier series are shown in figure 4(b). The amplitude of the $m = 2$ mode increases 0.5 ms after CTI, decreases after 2 ms before increasing again. The increase in the amplitude of magnetic fluctuations is due to the dominant $m = 2$ mode. It has been reported previously that CT injection into the CCW plasma current suppresses the $m = 2$ mode and does not have any effect on the $m = 3$ mode [6], different from the observation in the CW plasma current case.

The toroidal flow velocities of the three impurity ions, C_{III} , O_V and C_{VI} , for a discharge with the reversed (CW) plasma current direction are presented in figure 5. The positive vertical axis corresponds to the CCW direction, same as that in figure 2, or now the counter-current direction since the STOR-M discharge direction is reversed. During the discharge, a CT is injected at $t = 14.2$ ms. The average flow velocities of each of impurity ions over 15 STOR-M discharges without CTI are depicted with thin dashed lines. Before CT injection, the intrinsic toroidal flow velocity of C_{III} is negative, indicating a toroidal rotation in the CW direction or co-current direction.

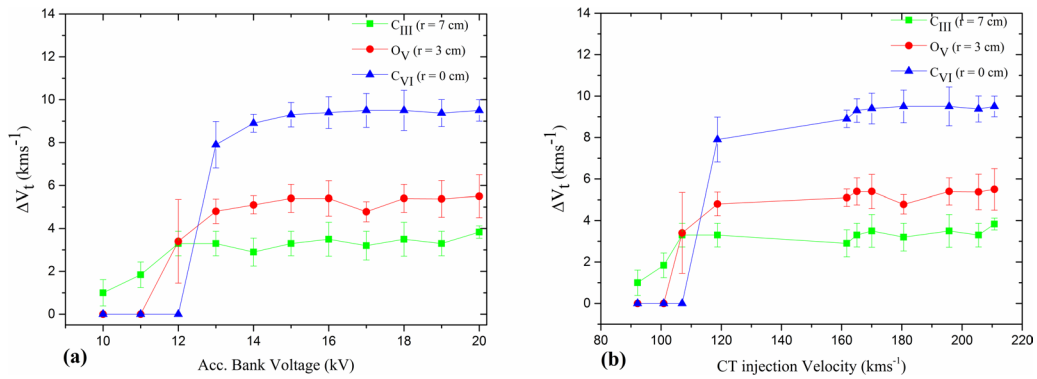


Figure 7. Toroidal rotational flow change for C_{III} ($r = 7 \text{ cm}$), O_V ($r = 3 \text{ cm}$) and C_{VI} ($r = 0 \text{ cm}$) ions with respect to the acceleration bank voltage of the CT injector (a), and the CT injection velocity (b).

These results suggest that the direction of toroidal flow at the outer region of the tokamak plasma is always in the direction of plasma current.

The toroidal flow velocity of C_{III} ions transiently changes its direction from -1.2 km s^{-1} (co-current) to 1.5 km s^{-1} (counter-current) or towards the CTI direction. Due to the high frequency and high amplitude noise immediately following CTI during this experimental campaign, the IDS data does not render reliable velocity information for about 0.8 ms and the possible trend is presented with dotted lines. When the plasma discharge current direction is reversed, the toroidal flow velocities of C_{VI} ions at the center and O_V ions near $r = 3 \text{ cm}$ reverse to positive, indicating a flow in the CCW or counter-current direction, as shown in figure 5. The toroidal flow velocity of O_V ions increases from 3.6 km s^{-1} to 10 km s^{-1} after CTI in the CCW direction. The flow change is still in the CTI direction. The toroidal flow velocity of C_{VI} ions in the plasma core increases from 12.5 km s^{-1} to 22 km s^{-1} . The change in the toroidal flow in the outer region at $r = 7 \text{ cm}$ is short-lived compared to the flow of impurities in the inner regions ($r = 3 \text{ cm}$ and $r = 0 \text{ cm}$).

It should be pointed out that the transit time of CT in STOR-M is on the order of $10 \mu\text{s}$, but the effects on the flow velocity last much longer on the order of a few milliseconds. Also, at different locations, the period with significant flow modification is different.

The flow shear in the core region is estimated by the difference between the flow velocity of the C_{VI} ions and that of C_{III} ions through $\Delta v/(r_{C_{III}} - r_{C_{VI}})$. The flow shear for both the CCW and CW plasma currents during the flattop without CTI is about $\sim 2 \text{ (km s}^{-1}\text{) cm}^{-1}$. After CTI, the flow shears for the CCW and CW plasma current are modified to $1.4 \text{ (km s}^{-1}\text{) cm}^{-1}$ and $3 \text{ (km s}^{-1}\text{) cm}^{-1}$, respectively. The improvement of confinement might be due to the enhancement of transport barriers caused by a sudden change in the toroidal flow shear after CTI [17].

It is clear that the flow shear is reduced for the normal (CCW) plasma current and enhanced for the reversed (CW) plasma current for a few milliseconds. CTI mainly affects the toroidal flow in the core region while its effect on the edge rotational flow is small and short lived. Furthermore, the toroidal flow direction in the core region is always in the counter-current direction regardless of the direction of the

STOR-M discharge current in the laboratory reference frame. As the direction of CTI remains unchanged and is always in the CCW direction, CTI slows down the rotational flow of the core region for the normal (CCW) current direction and speeds up for the reversed (CW) current direction while the change of flow at $r = 7 \text{ cm}$ towards the CTI direction is relatively small. In other words, the flow shear is decreased for the CCW current and increased for the CW current by CTI.

As shown in figures 2 and 6, the change of the toroidal flow velocity for the normal (CCW) plasma current lasts longer than that for the reversed (CW) current configuration. The reversal of the plasma current direction changes the direction of the magnetic field helicity of tokamak plasma while the direction of the magnetic helicity of CT remains unchanged. The magnetic reconnection process between the CT magnetic field and tokamak magnetic field is closely related to their helicity direction [18, 19]. The mechanism of modification of the toroidal flow by CTI might be also related to the magnetic reconnection process for deposition of the momentum.

The mass of CT is mainly controlled by the formation bank discharge, while the CT velocity is independently controlled by the bank voltage for the acceleration discharge as depicted in figure 1. However, the change in the tokamak plasma density (Δn_e) is related to the injection velocity (acceleration bank voltage) while the formation bank voltage remained unchanged (19 kV), as shown in figure 6. The change in tokamak plasma density increases by increasing the acceleration bank voltage for $V_{\text{acc}} < 15 \text{ kV}$. The kinetic energy of CT, which is responsible to overcome the magnetic barrier of the tokamak, is related to the injection velocity of CT. At higher injection velocities, CT is expected to penetrate deeper into the plasma and transfer more momentum to the tokamak plasma. However, the change in tokamak plasma density saturates at higher acceleration bank voltages ($> 15 \text{ kV}$). This saturation might be due to the increase of the CT mass loss in the CT acceleration region at high injection velocity as reported previously [18].

Figure 7 shows the change in the toroidal flow velocity of the impurity ions after CTI with respect to the acceleration bank voltage (figure 7(a)) and the CT velocity (figure 7(b)) of the CT injector. For low acceleration bank voltages (i.e. low CT injection velocities), there is little change in the flow velocity of C_{VI} ions which are concentrated at the core of

tokamak plasma. It is possible that the CT does not reach the core of the tokamak plasma at low injection velocities. For the flow of C_{III} ions at the outer region of the tokamak plasma, changes in the flow velocity have been observed at lower acceleration voltages. The flow velocity for all three impurity ions is saturated after $V_{acc} = 15$ kV. It was anticipated that momentum injection will be increased by increasing the injection velocity of the CT, but the results show the increase of the momentum injection does not follow the increase of the injection velocity of CT, possibly due to mass loss at high CT velocity which also limits the increase of the density in the tokamak discharge. There might be also other mechanisms for the saturation of the momentum injection at high CT injection velocities.

4. Summary and discussion

The toroidal flow of tokamak plasma plays a critical role in the plasma confinement and mitigation of disruption. NBI and RMP have been considered as rotational flow driver for tokamak plasma to enhance confinement. In this experimental campaign, the tokamak discharge current was reversed and the toroidal field direction remained intact. As expected, the intrinsic flow velocity direction was reversed. Since the RMP field no longer resonant with the target magnetic island, the modification of the flow velocity by RMP was insignificant, but was still towards the co-current direction. The CT injection direction was still in the CCW (or counter-current) direction. It was experimentally observed that the modification of the toroidal flow velocity was in the CT injection direction, or counter-current direction, suggesting that the modification of the flow velocity was due to the CT momentum injection. Although the CT injection time is on the order of $10 \mu s$, the modification of the flow velocity lasted several milliseconds. Experimental results showed the additional benefit of CT fuelling for future tokamak reactors. It has been shown that tangential CTI, beside the fuelling purpose, can be employed to control the rotational flow of tokamak plasma. It has been observed that the toroidal flow in STOR-M tokamak, despite the direction of plasma current, could be significantly modified by CTI. Furthermore, the IDS measurements have showed that the change in the toroidal flow in the core region after CTI was larger and lasted longer compared to the change in the outer region of the plasma. The enhancement of the rotational flow shear for the CW plasma current after CTI has been identified. The L-H and H-L transitions of confinement after CTI have been observed. It has been observed that the change in the toroidal flow and the line-averaged electron density of the tokamak plasma after CTI increased with

the CT velocity. However, for the injection velocities higher than 165 km s^{-1} , the change in the rotational flow saturated when injection velocity was further increased and the reason of the saturation of change in rotational flow is still unclear and requires further investigation. In addition, threshold of the CT velocity to influence the toroidal flow has also been observed.

Acknowledgments

This work was sponsored by the Natural Sciences and Engineering Research Council of Canada (NSERC), Canada Research Chair (CRC) program and the Sylvia Fedoruk Canadian Centre for Nuclear Innovation.

References

- [1] Raman R. and Gierszewski P. 1998 *Fusion Eng. Des.* **39–40** 977–85
- [2] Raman R. et al 1994 *Phys. Rev. Lett.* **73** 3101
- [3] Raman R. et al 2016 *J. Fusion Energy* **35** 34
- [4] Molvik A.W., Eddleman J.L., Hammer J.H., Hartman C.W. and McLean H.S. 1991 *Phys. Rev. Lett.* **66** 165–8
- [5] Onchi T., Liu Y., Dreval M., McColl D., Elgriw S., Liu D., Asai T., Xiao C. and Hirose A. 2013 *Plasma Phys. Control. Fusion* **55** 35003
- [6] Onchi T., McColl D., Rohollahi A., Xiao C., Hirose A., Dreval M. and Wolfe S. 2016 *IEEE Trans. Plasma Sci.* **44** 195–200
- [7] Xiao C. and Hirose A. 2004 *Phys. Plasmas* **11** 4041
- [8] Ware A.S., Terry P.W., Diamond P.H. and Carreras B.A. 1996 *Plasma Phys. Control. Fusion* **38** 1343–7
- [9] Ida K., Miura Y., Matsuda T., Itoh K., Hidekuma S., Itoh S.I. and JFT-2M Group 1995 *Phys. Rev. Lett.* **74** 1990–3
- [10] Elgriw S., Liu D., Asai T., Hirose A. and Xiao C. 2011 *Nucl. Fusion* **51** 113008
- [11] Elgriw S., Liu Y., Hirose A. and Xiao C. 2016 *Plasma Phys. Control. Fusion* **58** 045002
- [12] Xiao C., Liu D., Livingstone S., Singh A. K., Zhang A. and Hirose A. 2005 *Plasma Sci. Technol.* **7** 2701–4
- [13] Den Hartog D. J. and Fonk R. J. 1994 *Rev. Sci. Instrum.* **65** 3238
- [14] King J.D., McLean H.S., Wood R.D., Romero-Talamas C.A., Moller J.M. and Morse E.C. 2008 *Rev. Sci. Instrum.* **79** 10F535
- [15] Mitarai O., Xiao C., White D., McColl D., Zaawalski W. and Hirose A. 1997 *Rev. Sci. Instrum.* **68** 2711–6
- [16] Loewenhardt P.K., Brown M.R., Yee J. and Bellan P.M. 1995 *Rev. Sci. Instrum.* **66** 1050–5
- [17] Sen S., Xiao C., Hirose A. and Cairns R.A. 2002 *Phys. Rev. Lett.* **88** 185001
- [18] Perkins L.J., Ho S.K., Hammer J.H. 1998 *Nucl. Fusion* **28** 1365
- [19] Suzuki Y., Watanabe T. H., Sato T. and Hayashi T. 2000 *Nucl. Fusion* **40** 277–88